MOX–Report No. 12/2013

Mimetic finite differences for nonlinear and control problems

Antonietti, P.F.; Beirao da Veiga, L.; Bigoni, N.; Verani, M.

MOX, Dipartimento di Matematica "F. Brioschi"
Politecnico di Milano, Via Bonardi 9 - 20133 Milano (Italy)

mox@mate.polimi.it http://mox.polimi.it

Mimetic finite differences for nonlinear and control problems

Paola F. Antonietti[a], Lourenco Beirão da Veiga[b], Nadia Bigoni[c] and Marco Verani[d]

March 8, 2013

[a] MOX, Dipartimento di Matematica, Politecnico di Milano
Piazza Leonardo da Vinci 32, I-20133 Milano, Italy
E-mail: paola.antonietti@polimi.it

[b] Dipartimento di Matematica, Università di Milano
Via Saldini 50, I-20133 Milano, Italy
E-mail: lourenco.beirao@unimi.it

[c] MOX, Dipartimento di Matematica, Politecnico di Milano
Piazza Leonardo da Vinci 32, I-20133 Milano, Italy
E-mail: nadia.bigoni@mail.polimi.it

[d] MOX, Dipartimento di Matematica, Politecnico di Milano
Piazza Leonardo da Vinci 32, I-20133 Milano, Italy
E-mail: marco.verani@polimi.it

Abstract

In this paper we review some recent applications of the mimetic finite difference method to nonlinear problems (variational inequalities and quasilinear elliptic equations) and optimal control problems governed by linear elliptic partial differential equations. Several numerical examples show the effectiveness of mimetic finite differences in building accurate and robust numerical approximations. Finally, we draw some conclusions highlighting possible further applications of the mimetic finite difference method to nonlinear Stokes equations and shape optimization problems.

Keywords: Mimetic finite differences, nonlinear problems, control problems.

1 Introduction

Nowadays, the mimetic finite difference (MFD) method has become a very popular numerical approach to successfully solve a wide range of problems. This

is undoubtedly connected to its great flexibility in dealing with very general polygonal meshes and its capability of preserving the fundamental properties of the underlying physical and mathematical models (for a very restricted list see, for instance, [7–9,12,13,15–18,23] and the review paper [24] for a detailed introduction of the MFD method). The aim of this paper is to review some recent applications of the MFD method to nonlinear problems (variational inequalities and quasilinear elliptic equations) and constrained control problems governed by linear elliptic PDEs. In particular, we will show through several numerical examples the efficacy of mimetic finite differences in building accurate and robust numerical approximations. This is of paramount importance due to the ubiquitous presence of nonlinear and control problems in applied and industrial problems.

The outline of the paper is the following. In the next section we collect some useful notation and assumptions that will be employed throughout the paper. In Section 3 we consider the mimetic finite difference approximation of the obstacle problem, a paradigmatic example of variational inequality, while in Section 4 we consider the performance of the MFD method in approximating quasilinear elliptic problems. In Section 5 we turn the attention to the mimetic approximation of optimal control problems governed by linear elliptic equations. Finally, in Section 6 we highlight possible further applications of the MFD method to nonlinear Stokes equations and shape optimization problems, while in Section 7 we draw some conclusions.

2 Mesh assumptions and degrees of freedom

The aim of this section is to introduce some notation and the mesh assumptions, and to define the degrees of freedom for the discrete approximation spaces we are going to introduce later on. Throughout the paper, we will follow the usual notation for Sobolev spaces and norms (see e.g. [20]). Moreover, for any subset $\mathcal{D} \subseteq \mathbb{R}^2$ and non-negative integer k, we indicate by $\mathbb{P}_k(\mathcal{D})$ the space of polynomials of degree up to k defined on $\mathcal{D}$. Finally, we will use the symbol $\lesssim$ to indicate an upper bound that holds up to a positive multiplicative constant independent of h.

2.1 Mesh assumptions

Let Ω be a regular enough two-dimensional domain, and let Ω_h be a non-overlapping partition of Ω into, possibly non-convex, polygonal elements E with granularity $h = \sup_{E\in\Omega_h} h_E$, being h_E the diameter of $E \in \Omega_h$. We denote by $\mathcal{N}_h^\circ$ and $\mathcal{N}_h^\partial$ the sets of interior and boundary mesh vertices, respectively, and set $\mathcal{N}_h = \mathcal{N}_h^\circ \cup \mathcal{N}_h^\partial$. Proceeding as in [12] we also assume the following.

Assumption 2.1 (Mesh regularity assumptions) *There exist an integer number N and a shape regularity constant, both independent of h, such that for every*

element $E \in \Omega_h$ *it exists a compatible sub-decomposition* $\mathcal{T}_h^E$ *with at most* N shape-regular *triangles.*

We point out that Assumption 2.1 only requires the existence of a *compatible* sub-mesh that does not have to be constructed in practice. Moreover, it is easy to check that Assumption 2.1 guarantees that the following mesh regularity properties are satisfied

i) There exists $N_{\mathsf{e}} > 0$ such that every element E has at most N_{e} edges;

ii) There exists $\gamma > 0$ such that for every element E and for every edge e of E, it holds $|\mathsf{e}| \geq \gamma h_E$, where $|\mathsf{e}|$ is the length of e;

iii) For every $E \in \Omega_h$ and for every edge e of E, the following *trace inequality* holds

$$\|\psi\|^2_{L^2(\mathsf{e})} \lesssim h_E^{-1}\|\psi\|^2_{L^2(E)} + h_E\,|\psi|^2_{H^1(E)} \quad \forall\, \psi \in H^1(E).$$

2.2 Degrees of freedom for scalar and vector fields

In the following we will require to discretize scalar fields in $H^1(\Omega)$ and $L^2(\Omega)$, as well as vector fields in $H(\mathrm{div}, \Omega)$. Therefore, the scope of this section is to introduce the corresponding finite dimensional spaces V_h, Q_h, and X_h together with suitable interpolation operators from the continuous spaces to the associated discrete ones, and set up some notation.

We start defining the finite dimensional space V_h aiming at approximating the elements of $H^1(\Omega)$. Every discrete function $v_h \in V_h$ is a vector of real components $v_h = \{v^{\mathsf{v}}\}_{\mathsf{v}\in\mathcal{N}_h}$ one per mesh vertex, so that the dimension of V_h equals to the numbers of vertices of the mesh Ω_h. We also define V_h^g as the subset of V_h consisting of functions satisfying a Dirichlet-type boundary condition

$$V_h^g = \{v_h \in V_h \ : \ v_h^{\mathsf{v}} = g(\mathsf{v})\ \forall \mathsf{v} \in \mathcal{N}_h^{\partial}\},$$

with g a given smooth enough function. Accordingly, V_h^0 represents the space of discrete functions vanishing at the boundary nodes.

The space V_h is endowed with the following discrete seminorm

$$\|v_h\|^2_{1,h} = \sum_{E\in\Omega_h} \|v_h\|^2_{1,h,E} = \sum_{E\in\Omega_h} |E| \sum_{\substack{\mathsf{e}\in\mathcal{E}_h \\ \mathsf{e}\subset\partial E}} \left[\frac{1}{|\mathsf{e}|}(v^{\mathsf{v}_2} - v^{\mathsf{v}_1})\right]^2, \tag{1}$$

which becomes a norm in V_h^0. Here v_1 and v_2 are the two endpoints of $\mathsf{e} \in \mathcal{E}_h$, and $|E|$ is the area of the element $E \in \Omega_h$.

We define the following interpolation operator from the space $\mathcal{C}^0(\overline{\Omega}) \cap H^1(\Omega)$ into the discrete space V_h. For any $v \in \mathcal{C}^0(\overline{\Omega}) \cap H^1(\Omega)$, $v_{\mathrm{I}} \in V_h$ is defined as

$$v_{\mathrm{I}}^{\mathsf{v}} = v(\mathsf{v}) \quad \forall\, \mathsf{v} \in \mathcal{N}_h. \tag{2}$$

Notice that, under Assumption 2.1, the above interpolation operator satisfies classical approximation estimates, see [3]. The local version of the operator (2) is defined accordingly. That is, for any $v \in \mathcal{C}^0(\overline{E}) \cap H^1(E)$, $v_{\mathrm{I}} \in V_h|_E$ is given by

$$v_{\mathrm{I}}^{\mathsf{v}} = v(\mathsf{v}) \quad \forall\, \mathsf{v} \in \mathcal{N}_h^E,$$

with $\mathcal{N}_h^E$ the set of vertices of the polygon $E \in \Omega_h$.

Next we introduce the discrete space Q_h describing the degrees of freedom associated to a scalar field in $L^2(\Omega)$. Every discrete function $q_h \in Q_h$ is a vector of real components one per mesh cell, so that the dimension of Q_h equals the number of polygons in Ω_h. That is, for $q_h \in Q_h$ we have $q_h = \{q_E\}_{E\in\Omega_h}$, with $q_E \in \mathbb{R}$ the value of the discrete variable associated to the polygon $E \in \Omega_h$.

We endowed Q_h by the following scalar product

$$[p_h, q_h]_{Q_h} = \sum_{E\in\Omega_h} |E| p_E q_E \qquad \forall\, p_h, q_h \in Q_h, \tag{3}$$

and denote by $\|\cdot\|_{Q_h}$ the induced norm, i.e.,

$$\|p_h\|_{Q_h}^2 = [p_h, p_h]_{Q_h} \quad \forall\, p_h \in Q_h. \tag{4}$$

Notice that (3) coincide with the $L^2(\Omega)$ scalar product for piecewise constant functions.

For further use, we also introduce the following operator from $L^1(\Omega)$ onto Q_h

$$q_{\mathrm{I}}|_E = \frac{1}{|E|}\int_E q \; dV \quad \forall\, E \in \Omega_h \quad \forall\, q \in L^1(\Omega), \tag{5}$$

Finally, we introduce the finite dimensional space X_h aiming at approximating the elements of $H(\mathrm{div}, \Omega)$. In order to completely describe a vector field $G_h \in X_h$, we associate to any mesh edge $\mathsf{e} \in \mathcal{E}_h$ a real number $G_{\mathsf{e}} \in \mathbb{R}$, so that for $G_h \in X_h$, we have $G_h = \{G_{\mathsf{e}}\}_{\mathsf{e}\in\mathcal{E}_h}$. Clearly, the dimension of X_h is equal to the cardinality of $\mathcal{E}_h$.

The scalar product in X_h is defined by assembling elementwise contributions from each element, *i.e.*,

$$[F_h, G_h]_{X_h} = \sum_{E\in\Omega_h} [F_h, G_h]_E \quad \forall\, F_h, G_h \in X_h, \tag{6}$$

where the precise definition of $[\cdot,\cdot]_E$ will made be clear later on. The space X_h is equipped with the induced norm *i.e.*.

$$\|F_h\|_{X_h}^2 = [F_h, F_h]_{X_h} \quad \forall\, F_h \in X_h,$$

For any edge $\mathsf{e} \in \mathcal{E}_h$, we denote by $\mathbf{n}_{\mathsf{e}}$ the unit normal vector to $\mathsf{e} \in \mathcal{E}_h$ fixed once and for all, and define the projection operator from $H(\mathrm{div}, \Omega) \cap [L^s(\Omega)]^2$,

$s > 2$, onto X_h as follows

$$G_{\mathrm{I}}|_{\mathsf{e}} = \frac{1}{|\mathsf{e}|}\int_{\mathsf{e}} G\cdot\mathbf{n}_{\mathsf{e}}\, dS \quad \forall\, \mathsf{e}\in\mathcal{E}_h \quad \forall\, G\in H(\mathrm{div},\Omega), \tag{7}$$

Finally, we define the discrete divergence operator form the space X_h onto Q_h

$$\mathcal{DIV}_h : X_h \to Q_h \quad \mathcal{DIV}_h(G_h)|_E = \frac{1}{|E|}\sum_{\mathsf{e}\subseteq\partial E} |\mathsf{e}| G_{\mathsf{e}}^E \quad \forall E\in\Omega_h, \tag{8}$$

where $G_{\mathsf{e}}^E = G_{\mathsf{e}}\mathbf{n}_{\mathsf{e}}\cdot\mathbf{n}_{\mathsf{e}}^E \in \mathbb{R}$ and $\mathbf{n}_{\mathsf{e}}^E$ is the unit normal vector to e pointing outward to $E\in\Omega_h$. It is immediate to check that $\mathcal{DIV}_h(G_I) = (\mathrm{div}\, G)_I$ for all sufficiently regular vector fields G, where the first interpolation is in X_h and the second in Q_h.

The local bilinear forms (6) are defined as in [14] and satisfy the following two conditions:

(S1) *Continuity and coercivity*: For any $E\in\Omega_h$, it holds

$$\sum_{\mathsf{e}\subseteq\partial E} |E|(G_{\mathsf{e}}^E)^2 \lesssim [G_h, G_h]_E^2 \lesssim \sum_{\mathsf{e}\subseteq\partial E} |E|(G_{\mathsf{e}}^E)^2 \quad \forall G_h\in X_h.$$

(S2) *Local consistency*: for every linear function q^1 on $E\in\Omega_h$, it holds

$$[(\nabla q^1)_{\mathrm{I}}, G_h]_E + \int_E q^1\, \mathcal{DIV}_h(G_h)\, dV = \sum_{\mathsf{e}\subseteq\partial E} G_{\mathsf{e}}^E \int_{\mathsf{e}} q^1\, dS \quad \forall G_h\in X_h.$$

3 The obstacle problem

The aim of this section is to show that MFD methods can be successfully applied to discretize variational inequalities. To this aim we consider the simplest example, namely the obstacle problem which consists in finding the equilibrium position of an elastic membrane whose boundary is held fixed, and which is constrained to lie above a given obstacle. In the next Section we recall the continuous problem, then Section 3.2 is devoted to present the MFD discretization and the approximation results and finally Section 3.2 presents some numerical computations. Throughout this Section we will assume that the computational domain Ω is an open, bounded, convex set of $\mathbb{R}^2$, with either a polygonal or a C^2-smooth boundary.

3.1 Continuous problem

Let $\psi\in H^2(\Omega)$ a given function that satisfies $\psi\le g$ on $\partial\Omega$, where g is the trace of a given function in $H^2(\Omega)$, and let K be the convex set defined as

$$K = \{v\in H^1(\Omega)\ :\ v = g \text{ on } \partial\Omega \text{ and } v\ge\psi \text{ a.e. in } \Omega\}.$$

The obstacle problem can be written as the following variational inequality:

$$\text{Find } u \in K \text{ such that} \quad a(u, v-u) \geq F(v-u) \quad \forall v \in K, \tag{9}$$

respectively, where the bilinear form $a(\cdot,\cdot) : H^1(\Omega) \times H^1(\Omega) \longrightarrow \mathbb{R}$ and the linear functional $F(\cdot) : H^1(\Omega) \longrightarrow \mathbb{R}$ are defined as

$$a(u,v) = \int_\Omega \nabla u \cdot \nabla v \; dV, \quad F(v) = \int_\Omega f \; v \; dV, \tag{10}$$

with $f \in L^2(\Omega)$ a given function. It can be shown that under the above data regularity assumption, the elliptic obstacle problem (9) admits a unique solution $u \in H^2(\Omega)$, see e.g. [11] and [26, Corollary 5:2.3].

3.2 Discrete problem and convergence

We denote by $a_h(\cdot,\cdot) : V_h \times V_h \to \mathbb{R}$ the discretization of the bilinear form $a(\cdot,\cdot)$, defined as follows:

$$a_h(v_h, w_h) = \sum_{E \in \Omega_h} a_h^E(v_h, w_h) \quad \forall\, v_h, w_h \in V_h, \tag{11}$$

where $a_h^E(\cdot,\cdot) : V_h|_E \times V_h|_E \to \mathbb{R}$ are symmetric bilinear forms built on each element $E \in \Omega_h$ in such a way that the following properties are satisfied [12]

(S1) *Continuity and coercivity*: For every $u_h, v_h \in V_h$ and each $E \in \Omega_h$, we have

$$\|v_h\|_{1,h,E}^2 \lesssim a_h^E(v_h, v_h), \qquad a_h^E(u_h, v_h) \lesssim \|u_h\|_{1,h,E} \|v_h\|_{1,h,E}.$$

(S2) *Local consistency*: For every element E, every function $q^1 \in \mathbb{P}^1(E)$, and every $v_h \in V_h$, it holds

$$a_h^E(v_h, (q^1)_{\mathrm{I}}) = \sum_{\mathsf{e} \in \mathcal{E}_h^E} (\nabla q^1 \cdot \mathbf{n}_E^{\mathsf{e}}) \frac{|\mathsf{e}|}{2} \big(v_h^{\mathsf{v}_1} + v_h^{\mathsf{v}_2}\big),$$

where v_1 and v_2 are the two vertices of $\mathsf{e} \in \mathcal{E}_h$.

The meaning of the above consistency condition (S2) is that the discrete bilinear form respects integration by parts when tested with linear functions. The discretization of the load term is defined as

$$(f, v_h)_h = \sum_{E \in \Omega_h} \overline{f}|_E \sum_{i=1}^{k_E} v^{\mathsf{v}_i} \omega_E^i, \tag{12}$$

where $\mathsf{v}_1, \ldots, \mathsf{v}_{k_E}$ are the vertices of E, $\omega_E^1, \ldots, \omega_E^{k_E}$ are positive weights such that $\sum_{i=1}^{k_E} \omega_E^i = |E|$, and

$$\overline{f}|_E = \frac{1}{|E|} \int_E f \; dV.$$

Finally, we are able to define the proposed MFD method for the obstacle problem (9). Indeed, let us introduce the discrete convex space

$$K_h = \{v_h \in V_h^g \ : \ v_h^{\mathsf{v}} \geq \psi(\mathsf{v}) \ \forall \mathsf{v} \in \mathcal{N}_h\};$$

then the mimetic discretization of problem (9) reads:

$$\text{Find } u_h \in K_h \text{ such that} \quad a_h(u_h, v_h - u_h) \geq (f, v_h - u_h)_h \quad \forall v_h \in K_h. \tag{13}$$

It can be shown that problem (13) admits a unique solutions. Indeed, from property (S1), it is immediate to infer that the bilinear form $a_h(\cdot,\cdot)$ is coercive on $V_h/\mathbb{R}$. Then, the well posedness of (13) follows recalling that $K_h \subset V_h$ is convex and closed, and using standard results [20]. The following convergence result has been proved in [3].

Theorem 3.1 *Let $u \in K \cap H^2(\Omega)$ be the solution to the continuous problem (9), and $u_h \in K_h$ be the corresponding mimetic approximation obtained by solving the discrete problem (13). Then, it holds*

$$\|u_h - u_I\|_{1,h} \lesssim h.$$

3.3 Numerical results

We set $\Omega = (-1,1)^2$ and consider a variant of the example presented in [3]. Let $\psi(x,y) = 0$, and choose as exact solution of model problem (9)

$$u(x,y) = (\max\{x^2 + y^2 - r^2, 0\})^2, \tag{14}$$

with $r \in (0,1)$ a parameter at our disposal. Figure 1 depicts the minimizer u

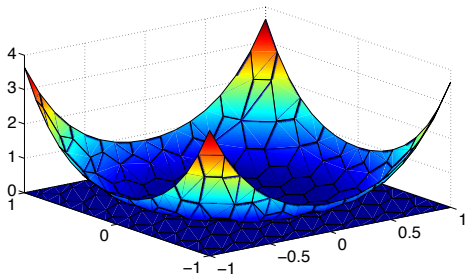

Figure 1: Obstacle problem. Exact solution u given in (14), $r = 0.3$, and the obstacle $\psi = 0$.

given in (14) together with the obstacle ψ in the case $r = 0.3$. The corresponding load $f(\cdot,\cdot)$ is given by

$$f(x,y) = \begin{cases} -8(2x^2 + 2y^2 - r^2) & \text{if } \sqrt{x^2+y^2} > r, \\ -8r^2(1 - x^2 - y^2 + r^2) & \text{if } \sqrt{x^2+y^2} \leq r, \end{cases}$$

and the Dirichlet boundary data $g(x,y) = (x^2+y^2-r^2)^2$. The obstacle problem (9) has been solved numerically by the Projected Successive Over Relaxation (PSOR) method (see [3] for more implementation details).

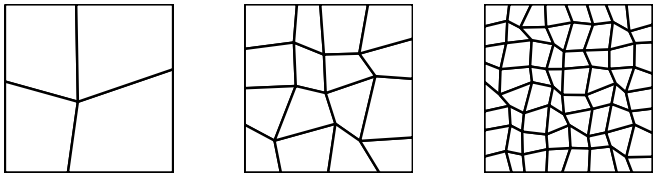

(a) *Quadrilateral* meshes. Refinement levels $\ell = 1, 2, 3$

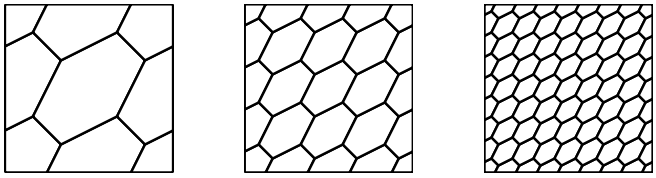

(b) *Media type-1* meshes. Refinement levels $\ell = 1, 2, 3$

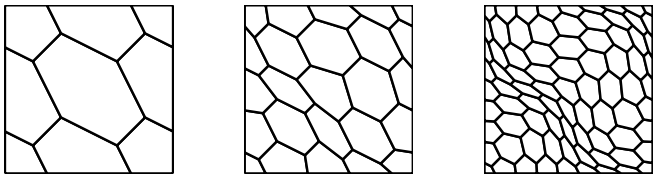

(c) *Media type-2* meshes. Refinement levels $\ell = 1, 2, 3$

Figure 2: Samples of *quadrilateral*, *median-type 1* and *median-type 2* decompositions of $\Omega = (-1,1)^2$. From left to right: refinement levels $\ell = 1, 2, 3$.

We have consider sequences of *quadrilateral*, *median-type 1* and *median-type 2* of decompositions as those shown in Figure 2 for the first three refinement levels $\ell = 1, 2, 3$. In Table 1 we report the errors $\|u_{\mathrm{I}} - u_h\|_{1,h}$ measured in the discrete energy norm defined in (1) for the considered sequence decompositions. In the last row of Table 1 we also report the computed convergence rates obtained by the linear regression algorithm. We can observe that on all the sequences of meshes a linear convergence rate is observed as predicted by Theorem 3.1. We refer to [4] for more numerical experiments including the numerical performance of an adaptive MFD method driven by a hierarchical a posteriori error estimator similar to the one proposed in [2].

Table 1: Obstacle problem. Computed errors $\|u_{\mathrm{I}} - u_h\|_{1,h}$ on the sequence of *quadrilateral*, *median-type 1* and *median-type 2* decompositions.

Refinement level	*quadrilateral*	*median-type 1*	*median-type 2*
$\ell = 1$	6.67435e-2	1.57514e-1	1.57514e-01
$\ell = 2$	6.04445e-2	6.71848e-2	6.20040e-02
$\ell = 3$	2.18688e-2	4.99534e-2	4.36785e-02
$\ell = 4$	1.04561e-2	2.55444e-2	1.95246e-02
$\ell = 5$	5.15400e-3	1.05753e-2	7.49375e-3
rate	0.99210	1.02879	1.04544

4 Quasilinear elliptic problems

The aim of this section is to show that the MFD method can be successfully employed to discretize quasilinear elliptic equations (see also, e.g., [1,10] for the finite volume approximation of nonlinear problems). In the following, we will recall the model problem under investigation, and its MFD discretization. The theoretical results reported below will also be validated by means of numerical experiments.

4.1 Continuous problem

In this section, we discuss the application of the MFD method for the approximation of the solution to the following quasilinear elliptic problem: Find $u \in H_0^1(\Omega)$ such that

$$b(u; u, v) = F(v) \quad \forall\, v \in H_0^1(\Omega), \tag{15}$$

where $f \in L^2(\Omega)$ is given function, $F(\cdot)$ is defined as in Section 10, and $b(\cdot;\cdot,\cdot)$ is a semilinear form defined as follows

$$b(u; v, w) = \int_\Omega \kappa(|\nabla u|^2)\, \nabla v \cdot \nabla w \; dV \quad \forall u, v, w \in H_0^1(\Omega). \tag{16}$$

The nonlinearity $\kappa : \mathbb{R}^+ \longrightarrow \mathbb{R}^+$ appearing in (16) is assumed to satisfy the following assumptions

i) $\kappa(\cdot)$ is continuous over $[0, +\infty)$;

ii) there exist two positive constants k_*, k^* such that:

$$k_*(t - s) \le \kappa(t^2)t - \kappa(s^2)s \le k^*(t - s) \quad \forall\, t > s \ge 0.$$

Among all the functions that satisfy the above conditions, we are particularly interested in the Carreau law

$$\kappa(t) = \eta_\infty + (\eta_0 - \eta_\infty)(1 + \lambda t)^{\frac{p-2}{2}}, \quad t \geq 0, \tag{17}$$

with $\eta_0 \geq \eta_\infty > 0$, $\lambda > 0$ and $p \in (1, 2)$. We recall that a fluid that obeys to a Carreau law is a type of generalized quasi-Newtonian fluid where viscosity depends upon the shear rate. For example, the rheologic behavior of many polymeric fluids or rubber-like liquids are frequently described in engineering literature by the Carreau law. Next, we briefly discuss the mimetic approximation of problem (15) and we refer to [6] for a more detailed discussion.

4.2 Discrete problem and convergence

Let us introduce an admissible partition Ω_h of the domain Ω, as explained in Section 2. In order to introduce a mimetic discretization of problem (15), we first consider the restriction of the form (16) on each element $E \in \Omega_h$, i.e.,

$$b^E(u; v, w) = \int_E \kappa(|\nabla u|^2) \nabla v \cdot \nabla w \; dV \quad \forall u, v, w \in H^1(E). \tag{18}$$

Observe that, whenever $\varphi \in \mathbb{P}^1(E)$, the local form $b^E(\varphi; \cdot, \cdot)$ can be rewritten as

$$b^E(\varphi; v, w) = \kappa(|\nabla \varphi|^2) \int_E \nabla v \cdot \nabla w \; dV \quad \forall\, \varphi \in \mathbb{P}^1(E) \quad \forall\, v, w \in H^1(E).$$

In view of the above relation, a MFD discretization of (18) can be obtained once that a suitable discrete approximation of the nonlinear term $\kappa(\cdot)$ and of the integral term $\int_E \nabla v \cdot \nabla w \, \mathrm{d}V$ are available. For the latter, we proceed exactly as in Section 3.2, by introducing the bilinear form (11) over the space V_h defined in Section 2.2. Therefore, we only have to discuss the MFD discretization of the nonlinear term $\kappa(\cdot)$ within each element $E \in \Omega_h$. Let us introduce the following operator

$$\mathcal{G}_h^E : V_h^E \longrightarrow \mathbb{R}^+ \quad \mathcal{G}_h^E(u_h) := \frac{a_h^E(u_h, u_h)}{|E|}, \tag{19}$$

on each $E \in \Omega_h$. Bearing in mind the fact that the bilinear form (11) is a discretization of the term $\int_E \nabla v \cdot \nabla w \, \mathrm{d}V$, the operator (19) turns out to be a good candidate to approximate $|\nabla u|^2$ within each element. Indeed,

$$\frac{\int_E |\nabla u|^2 \; dV}{|E|} \sim \mathcal{G}_h^E(u_{\mathtt{I}}) \quad \forall\, u \in H^1(E)$$

where the local interpolation operator $u_{\mathtt{I}} \in V_h|_E$ is defined according to (2) and the symbol $\sim$ stands for approximation. In view of the above discussion, we obtain the following mimetic discretization of the local form (18)

$$b_h^E(u_h; v_h, w_h) = \kappa(\mathcal{G}_h^E(u_h)) \; a_h^E(v_h, w_h) \quad \forall u_h, v_h, w_h \in V_h|_E.$$

Then, the discrete formulation of problem (15) reads: find $u_h \in V_h^0$, such that

$$b_h(u_h; u_h, v_h) = F_h(v_h) \quad \forall\, v_h \in V_h^0, \tag{20}$$

where

$$b_h(u_h; v_h, w_h) = \sum_{E \in \Omega_h} b_h^E(u_h; v_h, w_h) \quad \forall u_h, v_h, w_h \in V_h,$$

and where the right-hand-side of problem (20) is built as in (12).

In [6] it has been proved that the discrete problem (20) is well posed and that the following convergence result holds provided a suitable approximation property is satisfied. The validity of such assumption will be verified through numerical computations in Section 4.3.

Theorem 4.1 *Assume that the following approximation property holds: there exists $\alpha > 0$ so that*

$$\|\kappa(|\nabla v|^2) - \kappa(\mathcal{G}_h^E(v_I))\|_\infty \lesssim h^\alpha \quad \forall v \in H^1(\Omega). \tag{21}$$

Let $u \in H^2(\Omega) \cap H_0^1(\Omega)$ and $u_h \in V_h^0$ be the solutions of the continuous and discrete problems (15) *and* (20)*, respectively. Then, it holds*

$$\|u_I - u_h\|_{1,h} \lesssim h^{\min(1,\alpha)},$$

where u_I is the interpolation of the exact solution defined as in (2)*.*

4.3 Numerical results

We propose to solve the nonlinear problem (20) via linearization employing the Kačanov method. The *idealized* algorithm (*i.e.* without any stopping criterion) reads: given $u_h^{(0)} \in V_h^0$

$$\text{Find } u_h^{(k+1)} \in V_h^0 \text{ such that } b_h(u_h^{(k)}; u_h^{(k+1)}, v_h) = F_h(v_h) \quad \forall\, v_h \in V_h^0, \quad k \geq 0.$$

The convergence of the sequence $\{u_h^{(k)}\}_{k\geq 0}$ to the "exact" discrete solution u_h of problem (20) is stated in the following result. We refer to [6] for the proof.

Theorem 4.2 *Let $\{u_h^{(k)}\}_{k\geq 0}$ be the sequence built by the Kačanov method, then $u_h^{(k)} \longrightarrow u_h$ in V_h, as $k \to +\infty$.*

Next, we present a numerical example taken from [6], where we have employed the *feasible* Kačanov method supplemented with a suitable stopping criterion as described in Algorithm 4.1. The reliability of the stopping criterion employed in Algorithm 4.1 is discussed in [6] where it is also proposed a computable error indicator as a possible alternative strategy to stop the iterative scheme.

We suppose that the nonlinearity $\kappa(\cdot)$ obeys to the Carreau law (17), with $\eta_0 = 3$, $\eta_\infty = 1$ and $p = 1.7$. The source term f is selected so that $u(x, y) =$

Algorithm 4.1: *Feasible* Kačanov algorithm

Given the initial guess $u_h^{(0)}$, set `toll`, $k = -1$, $u_h^{(-1)} = u_h^{(0)}$;
while $\|u_h^{(k+1)} - u_h^{(k)}\|_{1,h} \geq$ `toll` **do**
  $k + 1 \leftarrow k$;
  `SOLVE` $b_h(u_h^{(k)}; u_h^{(k+1)}, v_h) = F_h(v_h) \quad \forall\, v_h \in V_h$;
end
`SET` $u_h = u_h^{(k+1)}$;

$x(1-x)y(1-y)(1-2y)\exp(-20((2x-1)^2))$ is the analytical solution of problem (20). We test our scheme on the same sequences of grids as the ones considered in Section 3.3, and throughout this section we set the tolerance `toll` equal to 10^{-8}.

In Table 2 we report the computed relative errors $\|u_{\mathtt{I}} - u_h\|_{1,h}/\|u_{\mathtt{I}}\|_{1,h}$ measured in the discrete energy norm (1) as a function of the refinement level ℓ. The last row of Table 2 also shows the computed convergence rate obtained by the linear regression algorithm. We observe that the error goes at a rate that is slightly better than predicted by our theoretical results given in Theorem 4.1, probably due to some improved convergence rate at the nodes of the mesh.

Finally, we present a numerical approach to validate hypothesis (21). Let us introduce the following discrete norm

$$\|v_h\|_{\infty,h} := \sup_{\mathtt{v} \in \mathcal{N}_h} |v_h^{\mathtt{v}}| \quad \forall v_h \in V_h,$$

and let us denote with Π^0 the projection onto the space of piecewise constant functions defined on Ω_h. By keeping in mind standard interpolation error estimates, hypothesis (21) can be validated by checking the numerical behavior of the following quantity

$$\left\| \kappa\left(\Pi^0 \left|\nabla u\right|^2\right) - \kappa(\mathcal{G}_h^E(u_{\mathtt{I}})) \right\|_{\infty,h},$$

where $u_{\mathtt{I}}$ is the interpolation of the exact solution. The numerical results are reported in Figure 3, from which the value $\alpha = 1$ can be guessed. Then, we can conclude that the optimal parameter α appearing in (21) can be set equal to one.

5 Optimal control problems

In this section we show the ability of the MFD method to approximate elliptic optimal control problems. In particular, we consider the following prototypal

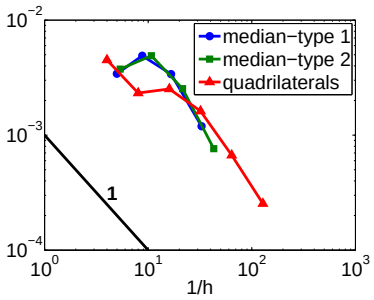

Figure 3: Quasi-linear elliptic problem and numerical validation of assumption (21): the behavior of $\|\kappa\left(\Pi^0 |\nabla u|^2\right) - \kappa(\mathcal{G}_h^E(u_{\mathrm{I}}))\|_{\infty,h}$ versus $1/h$ (loglog scale) is reported, with u denoting the exact solution.

Table 2: Quasi-linear elliptic problem. (Example taken from [6]) Computed relative errors $\|u_I - u_h\|_{1,h}/\|u_I\|_{1,h}$ in terms of the refinement level ℓ.

Refinement level	*median-type 1*	*median-type 2*	*quadrilateral*
$\ell = 1$	2.6147e+0	2.6147e+0	4.0053e-1
$\ell = 2$	1.1489e+0	1.0159e+0	1.7027e-1
$\ell = 3$	4.8404e-1	6.0820e-1	5.5403e-2
$\ell = 4$	1.8830e-1	2.3530e-1	1.6881e-2
$\ell = 5$	5.8092e-2	8.6861e-2	5.7466e-3
rate	1.5580	1.2843	1.2633

problem: find (F, y, u) such that

$$\begin{cases} \min\limits_{u\in K}\left\{\dfrac{1}{2}\|y-y^*\|^2_{L^2(\Omega)}+\dfrac{1}{2}\|F-F^*\|^2_{L^2(\Omega)}+\dfrac{\alpha}{2}\|u-u^*\|^2_{L^2(\Omega)}\right\} \\ \qquad F=-\nabla y \quad \text{in } \Omega, \\ \operatorname{div}(F)=f+u \quad \text{in } \Omega, \\ \qquad y=0 \qquad \text{on } \partial\Omega, \end{cases} \tag{22}$$

where K is a given convex subset of $L^2(\Omega)$, $f, y^*, u^* \in L^2(\Omega)$ and $F^* \in \left[L^2(\Omega)\right]^d$ are given functions and α is a positive real number.

5.1 Continuous problem

We start introducing the variational formulation of problem (22) that reads as follows. Find $(F, y, u) \in H(\operatorname{div}, \Omega) \times L^2(\Omega) \times K$ such that

$$\begin{cases} \min\limits_{u\in K}\left\{\dfrac{1}{2}\|y-y^*\|^2_{L^2(\Omega)}+\dfrac{1}{2}\|F-F^*\|^2_{L^2(\Omega)}+\dfrac{\alpha}{2}\|u-u^*\|^2_{L^2(\Omega)}\right\} \\ (F,G)_{L^2(\Omega)}-(y,\operatorname{div}(G))_{L^2(\Omega)}=0 \qquad \forall\, G\in H(\operatorname{div},\Omega), \\ (\operatorname{div}(F),q)_{L^2(\Omega)}=(f+u,q)_{L^2(\Omega)} \quad \forall\, q\in L^2(\Omega). \end{cases}$$

It is well known (see e.g., [22]) that the above problem admits a unique solution $(F, y, u) \in H(\operatorname{div}, \Omega) \times L^2(\Omega) \times K$ if and only if there exists $(P, z) \in H(\operatorname{div}, \Omega) \times L^2(\Omega)$ such that $(F, y, P, z, u) \in H(\operatorname{div}, \Omega) \times L^2(\Omega) \times H(\operatorname{div}, \Omega) \times L^2(\Omega) \times K$ satisfies the following optimality conditions:

$$\begin{cases} (F,G)_{L^2(\Omega)}-(y,\operatorname{div}(G))_{L^2(\Omega)}=0 & \forall\, G\in H(\operatorname{div},\Omega), \\ (\operatorname{div}(F),q)_{L^2(\Omega)}=(f+u,q)_{L^2(\Omega)} & \forall\, q\in L^2(\Omega), \\ (P,G)_{L^2(\Omega)}-(z,\operatorname{div}(G))_{L^2(\Omega)}=-(F-F^*,G)_{L^2(\Omega)} & \forall\, G\in H(\operatorname{div},\Omega), \\ (\operatorname{div} P,q)_{L^2(\Omega)}=(y^*-y,q)_{L^2(\Omega)} & \forall\, q\in L^2(\Omega), \\ (\alpha(u-u^*)-z,w-u)_{L^2(\Omega)}\geq 0 & \forall\, w\in K. \end{cases} \tag{23}$$

5.2 Discrete problem and convergence

Let X_h and Q_h be defined as in Section 2, and suppose that $K_h \subseteq Q_h$ is a closed subset of Q_h, then the discrete formulation of problem (23) is easily obtained as follows: Find $(F_h, y_h, P_h, z_h, u_h) \in X_h \times Q_h \times X_h \times Q_h \times K_h$ such that

$$\begin{cases} [F_h,G_h]_{X_h}-[y_h,\mathcal{DIV}_h(G_h)]_{Q_h}=0 & \forall\, G_h\in X_h, \\ [\mathcal{DIV}_h(F_h),\boldsymbol{q}]_{Q_h}=[f_{\mathrm{I}}+u_h,q_h]_{Q_h} & \forall\, q_h\in Q_h, \\ [P_h,G_h]_{X_h}-[z_h,\mathcal{DIV}_h(G_h)]_{Q_h}=-[F_h-F^*_{\mathrm{I}},G_h]_{X_h} & \forall\, G_h\in X_h, \\ [\mathcal{DIV}_h(P_h),\boldsymbol{q}]_{Q_h}=[y^*_{\mathrm{I}}-y_h,q_h]_{Q_h} & \forall\, q_h\in Q_h, \\ [\alpha\,(u_h-u^*_{\mathrm{I}})-z_h,w_h-u_h]_{Q_h}\geq 0 & \forall\, w_h\in K_h\ , \end{cases} \tag{24}$$

where $f_{\rm I}$, $y^*_{\rm I}$, $F^*_{\rm I}$ and of $u^*_{\rm I}$ are the interpolation of f, y^*, F^* and of u^*, respectively, defined according to (5) and (7), and $\mathcal{DIV}_h$ is the discrete divergence operator defined in (8). Moreover, we can state the following *a-priori* error estimates for the MFD discretization of problem (23) which has been proved in [5].

Theorem 5.1 *Let $(F, y, P, z, u) \in X \times Q \times X \times Q \times K$ be the exact optimal solution to* (23) *and let $(F_h, y_h, P_h, z_h, u_h) \in X_h \times Q_h \times X_h \times Q_h \times K_h$ be the discrete optimal solution to* (24)*. Then,*

$$\|u_I - u_h\|_{Q_h} \lesssim h,$$

where $u_I \in Q_h$ is the projection of u as defined in (5) *and*

$$\begin{aligned} \|F_I - F_h\|_{X_h} + \|y_I - y_h\|_{Q_h} &\lesssim h, \\ \|P_I - P_h\|_{X_h} + \|z_I - z_h\|_{Q_h} &\lesssim h \ , \end{aligned}$$

where $y_I, z_I \in Q_h$ are the projection of y and z, respectively, defined as in (5)*, and $F_I, P_I \in X_h$ are the interpolants of F and P, respectively, defined according to* (7)*.*

We recall that the above estimates can be extended analogously to high-order MFD method (see [5]).

5.3 Numerical results

The numerical example presented in this section has been performed again on the *quadrilateral*, *median-type 1* and *median-type 1* decompositions of the domain $\Omega = (0,1)^2$ as the ones shown in Figure 2. The optimization problem has been solved numerically by using the Primal-Dual strategy and the constant α appearing in the optimality conditions (23) has been set equal to 1. We have chosen

$$y^* = (1 - 2\pi^2)y \quad F^* = -\nabla y, \quad u^* = \exp(x_1^2 + x_2^2)\sin(5\pi x_1) + \sin(5\pi x_2),$$

and $f = -\Delta y - u$, so that the exact solution (F, y, P, z, u) of problem (23) is given by:

$$\begin{aligned} y &= \sin(\pi x_1)\sin(\pi x_2), \quad & z &= -\sin(\pi x_1)\sin(\pi x_2), \quad & u &= \max(u^* + z, 0), \\ F &= -\nabla y, & P &= -\nabla z. \end{aligned}$$

In Figure 4 (loglog scale) we report the errors $\|y_{\rm I} - y_h\|_{Q_h}$, $\|z_{\rm I} - z_h\|_{Q_h}$, $\|u_{\rm I} - u_h\|_{Q_h}$ computed in the discrete energy norm defined in (4) versus $1/h$. We can observe that the errors of the primal and the dual variables y and z go to zero quadratically, whereas for the control variable z we observe a convergence rate equal to $3/2$ as the mesh-size h goes to zero. Moreover, let us recall that the error estimates given in Theorem 5.1 predict a linear convergence rate for all of the variables, while the computed rates seems to be at least half order better

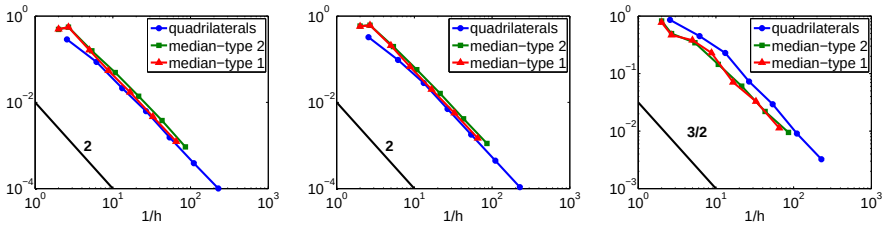

(a) $\|y_{\mathrm{I}} - y_h\|_{Q_h}$ (b) $\|z_{\mathrm{I}} - z_h\|_{Q_h}$ (c) $\|u_{\mathrm{I}} - u_h\|_{Q_h}$

Figure 4: Optimal control problem. Computed errors $\|y_{\mathrm{I}} - y_h\|_{Q_h}$, $\|z_{\mathrm{I}} - z_h\|_{Q_h}$, $\|u_{\mathrm{I}} - u_h\|_{Q_h}$ versus $1/h$ (loglog scale).

than predicted. For a similar problem in the finite element context, such a superconvergence phenomenon has already been observed in [19], where a proof of this behavior for the case of the lowest order Raviart-Thomas elements is presented.

6 Perspectives

In this section, we will shortly present two very recent lines of investigation naturally stemming from the problems and the techniques considered in this review. In particular, hinging upon the mimetic solver for quasilinear elliptic problems, in Section 6.1 we explore the numerical performance of the MFD method to approximate a nonlinear Stokes equation. Finally, in Section 6.2 we explore the capability of the MFD method to deal with very general polygonal decomposition by considering the mimetic approximation of a control problem where the control variable is represented by the computational domain; in particular, we will solve a simple shape optimization problem governed by a linear elliptic equation.

6.1 Nonlinear Stokes problems

In this subsection, we briefly describe the numerical performance of the MFD method for the approximation of the solution of the following nonlinear Stokes problem

$$\begin{cases} -\mathbf{div}\left(\kappa\left(|\boldsymbol{\epsilon}(\mathbf{u})|^2\right)\boldsymbol{\epsilon}(\mathbf{u})\right) + \nabla p = \mathbf{f} & \text{in } \Omega \\ \operatorname{div}\mathbf{u} = 0 & \text{in } \Omega \\ \mathbf{u} = 0 & \text{on } \partial\Omega, \end{cases} \tag{25}$$

where $\boldsymbol{\epsilon}(\mathbf{u}) = \frac{\nabla\mathbf{u}+\nabla\mathbf{u}^T}{2}$ is the symmetric gradient operator and the nonlinear function $\kappa(\cdot)$ obeys the *Carreau law*, i.e.

$$\kappa(|\epsilon(\mathbf{u})|) = \eta_\infty + (\eta_0 - \eta_\infty)(1 + \lambda|\epsilon(\mathbf{u})|^2)^{\frac{p-2}{2}},$$

with $\eta_0 \geq \eta_\infty > 0$, $\lambda > 0$ and $p \in (1,2)$. The above nonlinear Stokes problem (25) is approximated by resorting to the Uzawa's iterative method which requires the solution of a quasilinear elliptic problem at each iteration. The latter is addressed by employing the MFD method that is an extension of the scheme in Section 4. Without addressing the details, we just mention that we search for $u_h \in [V_h]^2$ and $p_h \in Q_h$.

In the following, we present a numerical example where the exact solution $(\mathbf{u}, p)$ of problem (25) is set chosen as

$$\mathbf{u} = [-\cos(2\pi x)\sin(2\pi y) + \sin(2\pi y), \sin(2\pi x)\cos(2\pi y) - \sin(2\pi x)]$$
$$p = 2\pi(\cos(2\pi y) - \cos(2\pi x)).$$

In Figure 5 (loglog scale) we report, for the set of computational meshes depicted in Figure 2, the computed errors $\|p_{\mathtt{I}} - p_h\|_{Q_h}$ and $\|\mathbf{u}_{\mathtt{I}} - \mathbf{u}_h\|_{1,h}$ versus the meshsize h. Here, $(\mathbf{u}_h, p_h)$ denotes the exact discrete solution, $(p_{\mathtt{I}}, \mathbf{u}_{\mathtt{I}})$ are the interpolations of the exact continuous solution defined as in Section 2.2, $\|\cdot\|_{1,h}$ is the energy norm defined as in (1), and $\|\cdot\|_{Q_h}$ is the mesh-dependent norm introduced in (4).

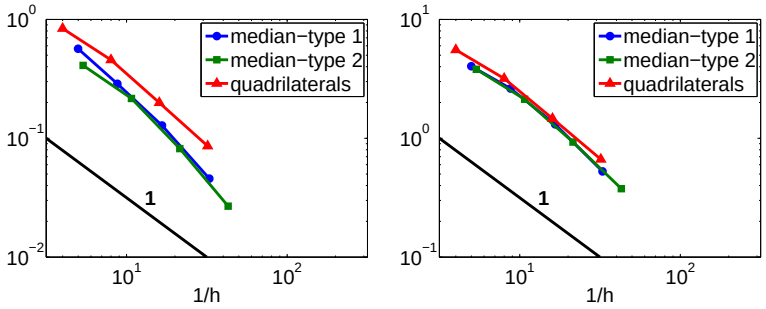

(a) $\|p_{\mathtt{I}} - p_h\|_{Q_h}$ (b) $\|\mathbf{u}_{\mathtt{I}} - \mathbf{u}_h\|_{1,h}$

Figure 5: Nonlinear Stokes problem: MFD discretization of problem (25). Computed errors versus $1/h$.

We observe that in all the cases errors converge linearly to zero, as the mesh size h goes to zero.

6.2 Shape optimization problems

In this section, we apply the MFD method to solve a simple shape optimization problem of the form:

$$\text{find } \Omega^* \in \mathcal{U}_{ad} : \mathcal{J}(\Omega^*, y(\Omega^*)) = \inf_{\Omega \in \mathcal{U}_{ad}} \mathcal{J}(\Omega, y(\Omega)),$$

where $\mathcal{J}$ is a given cost functional, $\mathcal{U}_{ad}$ is the set of admissible domains in $\mathbb{R}^2$ and $y(\Omega)$ is the solution of an elliptic equation on Ω. In this context, the crucial issue in obtaining reliable numerical simulations is to correctly handle the

deformation of the computational domain that usually requires a massive use of re-meshing techniques to preserve mesh regularity (see e.g. [25]). Here, we show that the MFD method represents a very promising technology to solve shape optimization problems, without resorting to any re-meshing strategy, since the MFD method can naturally deal with meshes made of very general polygons.

In the following, we consider the benchmark problem introduced in [21]. In particular, we consider the domain $\Omega \subset \mathbb{R}^2$ with $\partial\Omega = \Gamma \cup \Sigma_1 \cup \Sigma_2$ as depicted in Figure 6. Moreover, let D be an open bounded subset of Ω. The set $\mathcal{U}_{ad}$ of admissible domains contains all domains obtained through a deformation of Ω by keeping Σ_1 and Σ_2 fixed and by moving only Γ in such a way that $\Gamma \cap D = \emptyset$. We define the cost functional as follows

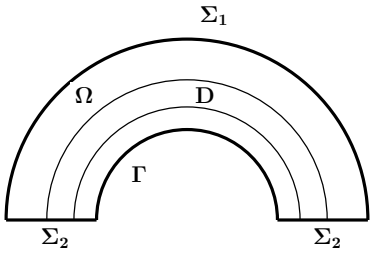

Figure 6: Computational domain for the optimization problem (26)-(27).

$$\mathcal{J}(\Omega, y(\Omega)) := \frac{1}{2}\int_D (y(\Omega) - z_g)^2 \; dV + \frac{\gamma}{2}\left(\int_\Gamma \; dS - P\right)^2, \tag{26}$$

where $\gamma > 0$ is a penalization parameter for the length of the moving boundary Γ, P is a target value for the perimeter, $z_g : D \to \mathbb{R}$ is a given function and $y(\Omega)$ is the solution of the following elliptic problem on Ω

$$-\Delta y = 0 \quad \text{in } \Omega, \quad y = 0 \quad \text{on } \Sigma_1, \quad \partial_n y = 0 \quad \text{on } \Sigma_2, \quad \partial_n y = 1 \quad \text{on } \Gamma. \tag{27}$$

Let $\mathbf{x} = (x_1, x_2)$, and let $\|\cdot\|$ denote the Euclidean norm. In the numerical test, we choose the region D equal to the half ring $\{2 \le \|\mathbf{x}\| \le 2.5\} \cap \{x_2 > 0\}$ and z_g is the exact solution of (27) on $\Omega = \{1 < \|\mathbf{x}\| < 3\} \cap \{x_2 > 0\}$. We point out that a global minimizer exists and it is exactly $\Omega^* = \{1 < \|\mathbf{x}\| < 3\} \cap \{x_2 > 0\}$.

In Figure 7 we report the starting computational domain Ω_0 and the final optimal computational domain obtained after four iterations of a steepest-descent like algorithm (see e.g. [21] for more details). In the algorithm, we solve problem (27) using the mixed MFD method as in Section 5.2, see also [13,15]. Boundary conditions are suitably modified to include the Neumann term.

In Figure 8 (right) we report the convergence history in terms of the iteration numbers. We can observe that the deformation of the elements close to

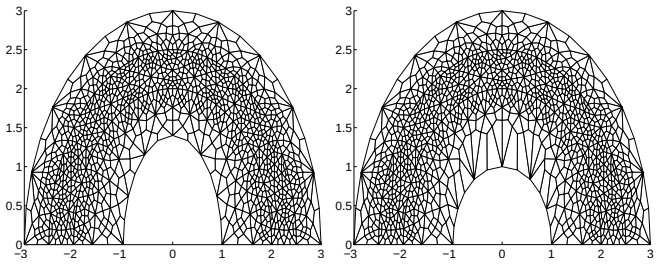

Figure 7: Shape optimization problem. Starting computational domain Ω_0 (left) and final one Ω_4 (right) obtained after four iterations.

the moving boundary (see Figure 8 (left)) does not affect the efficiency of the algorithm. Therefore, re-meshing technique seem not to be necessary when using the MFD method for solving shape optimization problems. This issue will be the object of further investigations.

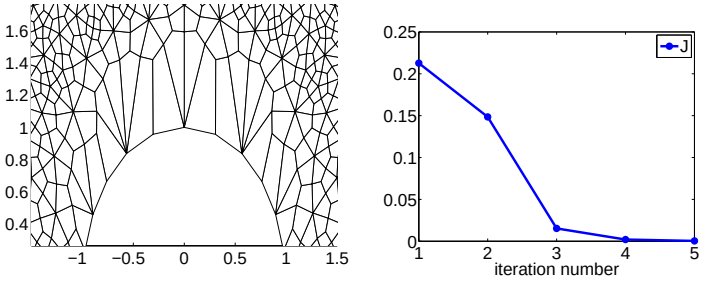

Figure 8: Shape optimization problem. Final domain Ω_4: zoom on the distorted elements of the computational grid (left). Convergence history in terms of the number of iteration (right)

7 Conclusions

In this paper we reviewed some recent applications of the MFD method to nonlinear problems (variational inequalities and quasilinear elliptic equations) and constrained control problems governed by linear elliptic PDEs. In all these cases we showed the efficacy of mimetic finite differences in building accurate and robust numerical approximations. We also presented two very recent lines of investigation naturally stemming from the problems and the techniques considered in this review, namely the impact of the MFD method on the approximate solution of nonlinear Stokes equations and shape optimization problems.

References

[1] B. Andreianov, F. Boyer, and F. Hubert. Discrete duality finite volume schemes for Leray-Lions-type elliptic problems on general 2D meshes. *Numer. Methods Partial Differential Equations*, 23(1):145–195, 2007.

[2] P. Antonietti, L. Beirão da Veiga, C. Lovadina, and M. Verani. Hierarchical a posteriori error estimators for the mimetic discretization of elliptic problems. *SIAM J. Numer. Anal.*, 51(1):654–675, 2013.

[3] P. F. Antonietti, L. Beirão da Veiga, and M. Verani. A mimetic discretization of elliptic obstacle problems. *Math. Comp.*, published online 20 Feb 2013.

[4] P. F. Antonietti, L. Beirão da Veiga, and M. Verani. Numerical performance of an adaptive mfd method for the obstacle problem. In *Numerical Mathematics and Advanced Applications. Proceedings of the 9th European Conference on Numerical Mathematics and Advanced Applications, Springer Verlag Italia*. Springer, Berlin, 2013.

[5] P. F. Antonietti, N. Bigoni, and M. Verani. Mimetic discretizations of elliptic control problems. *Journal of Scientific Computing*, 2012. doi: 10.1007/s10915-012-9659-7.

[6] P. F. Antonietti, N. Bigoni, and M. Verani. Mimetic finite difference approximation of quasilinear elliptic problems. Technical Report MOX-Preprint, 38/2012. Submitted for publication, 2012.

[7] L. Beirão da Veiga. A residual based error estimator for the mimetic finite difference method. *Numer. Math.*, 108(3):387–406, 2008.

[8] L. Beirão da Veiga, F. Brezzi, A. Cangiani, G. Manzini, L. D. Marini, and A. Russo. Basic principles of virtual element methods. *Math. Models Methods Appl. Sci.*, 23:119–214, 2013.

[9] L. Beirão da Veiga, K. Lipnikov, and G. Manzini. Convergence analysis of the high-order mimetic finite difference method. *Numer. Math.*, 113(3):325–356, 2009.

[10] F. Boyer and F. Hubert. Finite volume method for 2D linear and nonlinear elliptic problems with discontinuities. *SIAM J. Numer. Anal.*, 46(6):3032–3070, 2008.

[11] H. R. Brezis and G. Stampacchia. Sur la régularité de la solution d'inéquations elliptiques. *Bull. Soc. Math. France*, 96:153–180, 1968.

[12] F. Brezzi, A. Buffa, and K. Lipnikov. Mimetic finite differences for elliptic problems. *M2AN Math. Model. Numer. Anal.*, 43(2):277–295, 2009.

[13] F. Brezzi, K. Lipnikov, and M. Shashkov. Convergence of the mimetic finite difference method for diffusion problems on polyhedral meshes. *SIAM J. Numer. Anal.*, 43(5):1872–1896 (electronic), 2005.

[14] F. Brezzi, K. Lipnikov, and M. Shashkov. Convergence of mimetic finite difference method for diffusion problems on polyhedral meshes with curved faces. *Math. Models Methods Appl. Sci.*, 16(2):275–297, 2006.

[15] F. Brezzi, K. Lipnikov, and V. Simoncini. A family of mimetic finite difference methods on polygonal and polyhedral meshes. *Math. Models Methods Appl. Sci.*, 15(10):1533–1551, 2005.

[16] A. Cangiani, F. Gardini, and G. Manzini. Convergence of the mimetic finite difference method for eigenvalue problems in mixed form. *Comput. Methods Appl. Mech. Engrg.*, 200(9-12):1150–1160, 2011.

[17] A. Cangiani and G. Manzini. Flux reconstruction and pressure post-processing in mimetic finite difference methods. *Comput. Methods Appl. Mech. Engrg.*, 197/9-12:933–945, 2008.

[18] A. Cangiani, G. Manzini, and A. Russo. Convergence analysis of the mimetic finite difference method for elliptic problems. *SIAM J. Numer. Anal.*, 47(4):2612–2637, 2009.

[19] Y. Chen, Y. Huang, W. Liu, and N. Yan. Error estimates and superconvergence of mixed finite element methods for convex optimal control problems. *J. Sci. Comput.*, 42(3):382–403, 2010.

[20] P. G. Ciarlet. *The finite element method for elliptic problems.* North-Holland Publishing Co., Amsterdam, 1978. Studies in Mathematics and its Applications, Vol. 4.

[21] G. Doğan, P. Morin, R. H. Nochetto, and M. Verani. Discrete gradient flows for shape optimization and applications. *Comput. Methods Appl. Mech. Engrg.*, 196(37-40):3898–3914, 2007.

[22] J.-L. Lions. *Optimal control of systems governed by partial differential equations.* Translated from the French by S. K. Mitter. Die Grundlehren der mathematischen Wissenschaften, Band 170. Springer-Verlag, New York, 1971.

[23] K. Lipnikov, G. Manzini, F. Brezzi, and A. Buffa. The mimetic finite difference method for the 3D magnetostatic field problems on polyhedral meshes. *J. Comput. Phys.*, 230(2):305–328, 2011.

[24] K. Lipnikov, G. Manzini, and M. Shashkov. Mimetic finite difference method. Review paper, submitted for publication.

[25] P. Morin, R. Nochetto, M. Pauletti, and M. Verani. Adaptive finite element method for shape optimization. *ESAIM - Control, Optimisation and Calculus of Variations*, 18(4):1122–1149, 2012.

[26] J.-F. Rodrigues. *Obstacle problems in mathematical physics*, volume 134 of *North-Holland Mathematics Studies*. North-Holland Publishing Co., Amsterdam, 1987. Notas de Matemática [Mathematical Notes], 114.

MOX Technical Reports, last issues

Dipartimento di Matematica "F. Brioschi",
Politecnico di Milano, Via Bonardi 9 - 20133 Milano (Italy)

12/2013 Antonietti, P.F.; Beirao da Veiga, L.; Bigoni, N.; Verani, M.
Mimetic finite differences for nonlinear and control problems

11/2013 Discacciati, M.; Gervasio, P.; Quarteroni, A.
The Interface Control Domain Decomposition (ICDD) Method for Elliptic Problems

10/2013 Antonietti, P.F.; Beirao da Veiga, L.; Mora, D.; Verani, M.
A stream virtual element formulation of the Stokes problem on polygonal meshes

09/2013 Vergara, C.; Palamara, S.; Catanzariti, D.; Pangrazzi, C.; Nobile, F.; Centonze, M.; Faggiano, E.; Maines, M.; Quarteroni, A.; Vergara, G.
Patient-specific computational generation of the Purkinje network driven by clinical measuraments

08/2013 Chen, P.; Quarteroni, A.; Rozza, G.
A Weighted Reduced Basis Method for Elliptic Partial Differential Equations with Random Input Data

07/2013 Chen, P.; Quarteroni, A.; Rozza, G.
A Weighted Empirical Interpolation Method: A-priori Convergence Analysis and Applications

06/2013 Ded, L.; Quarteroni, A.
Isogeometric Analysis for second order Partial Differential Equations on surfaces

05/2013 Caputo, M.; Chiastra, C.; Cianciolo, C.; Cutri , E.; Dubini, G.; Gunn, J.; Keller, B.; Zunino, P.;
Simulation of oxygen transfer in stented arteries and correlation with in-stent restenosis

04/2013 Morlacchi, S.; Chiastra, C.; Cutr, E.; Zunino, P.; Burzotta, F.; Formaggia, L.; Dubini, G.; Migliavacca, F.

Stent deformation, physical stress, and drug elution obtained with provisional stenting, conventional culotte and Tryton-based culotte to treat bifurcations: a virtual simulation study

03/2013 Antonietti, P.F.; Ayuso de Dios, B.; Bertoluzza, S.; Pennacchio, M.
Substructuring preconditioners for an $h-p$ Nitsche-type method